Proceedings of the ASME 2016 35th International Conference on Ocean, Offshore and Arctic Engineering
OMAE2016
June 19-24, 2016, Busan, South Korea

OMAE2016-54915

Comparing a fracture mechanics model to the SN-curve approach for jacket-supported offshore wind turbines: Challenges and opportunities for lifetime prediction

Lisa Ziegler
Ramboll Wind, Hamburg, Germany
Norwegian University of Science and Technology
Trondheim, Norway

Michael Muskulus
Norwegian University of Science and Technology
Trondheim, Norway

ABSTRACT

Accurate lifetime predictions are needed for support structures of offshore wind turbines to optimize operation and maintenance and to decide about lifetime extension of aging wind farms. A comparison of a facture mechanics model to the SN-curve approach for jacket supported offshore wind turbines shows that it is attractive for lifetime extension decisions; however major challenges are calibration of material parameters and assumptions for initial crack size. Crack growths on a Y-joint connecting brace and jacket leg was analysed with simulations of structural response to aero- and hydrodynamic loading and Paris' law for crack propagation. The model was calibrated to yield an identical fatigue life as obtained from the SN-curve analysis. The effect of weather seasonality on crack growth was evaluated with a Markov weather model and Monte Carlo simulations. Results show that crack growth is sensitive to parameter calibration and follows seasonal weather trends.

KEYWORDS: fatigue, crack growth, offshore wind turbine, fracture mechanics, seasonality

1. INTRODUCTION

1.1 Motivation

Offshore wind energy has developed rapidly in the past two decades - from small near shore wind farms in less than 10m water depth up to large turbines (>5 MW) in deeper water today [1]. Jackets are common support structures for offshore wind turbines (OWT) installed in the transition zone between moderate water depth (<30 m), where monopiles are predominant foundations, and deep water (>50 m), where floating structures are necessary [2]. The most important challenge for commissioned wind energy projects is to keep reliability and profitability through well-organized operation and maintenance procedures [3]. In addition, profit can be increased by extending the operation of safe and economic wind farms beyond their original design lifetime of 20-25 years. For both purposes, accurate prediction of the health and remaining useful lifetime of all OWT components is needed. A crucial factor is structural integrity of support structures since an unpredicted tower or foundation failure, such as recently happened to one OWT in the Samsø Offshore Wind Farm [4], leads to a large loss on investment.

1.2 Support structure design and lifetime prediction

Design of OWT support structures is complex since it has to account for a large number of environmental conditions and loading scenarios during 20-25 years of wind farm operation [5]. Fatigue is often a design driver for OWT support structures since they are subjected to long-term cyclic loadings from wind, waves and current.

After some years in operation, the consumed lifetimes of jacket support structures often differ from design lifetimes due to large uncertainties in environmental loading, material resistance, and design models. In addition, variation of site conditions in large wind farms lead to differences in the load level between turbines [6]. Updating calculated lifetimes is crucial for scheduling inspections and to decide about lifetime extension of OWTs. A main element in lifetime prediction is the fatigue damage model, typically based on a SN-curve or alternatively linear-elastic fracture mechanics approaches.

Fracture mechanic models are advanced compared to SN-curve approaches since they offer detailed crack growth description. However, substantial practical problems, for example, model complexity and the uncertainty in material parameters, limit the use of fracture mechanic models for design of OWT support structures nowadays. However, DNV GL [7] recommends fracture mechanics approaches for assessment of (I) occurred fatigue cracks, (II) fabrication quality criteria, and

(III) inspection planning, where simplified SN-curve models do not give sufficient information.

1.3 Scope of this work

The intention of this paper is to discuss the applicability of a linear-elastic fracture mechanics model for the issue of lifetime prediction for offshore wind jackets. The focus is on fatigue crack growth at a Y-joint connecting a jacket brace to a leg. The opportunities and challenges evolving from modelling crack growth during design and operation are reviewed and compared to the SN-curve approach. This paper applies a simplified fracture mechanics model with the analytical formulation of Paris' law for crack growth, but does not go into details regarding finite element analysis for the calibration of stress intensity factors. The effect of weather seasonality on fatigue crack growths is assessed and different approaches for parameter calibration are discussed.

The remainder of this paper is organized as follows. First, Section 2 outlines fracture mechanic models and fatigue design with SN-curves. The numerical wind turbine model and simulated load cases for the structural analysis are introduced. Furthermore, a brief summary of a persistent weather model is given. Results of crack growth simulations are presented in Section 3, while Section 4 provides a discussion on challenges and opportunities for lifetime prediction. Finally, the paper is ended with conclusions in Section 5.

1.4 State of the art

Linear-elastic fracture mechanics models have been extensively discussed for marine structures in the oil & gas industry, mostly focusing on tubular joints [8–10]. Kirkemo [9] gives a comprehensive introduction to probabilistic fracture mechanics for offshore structures. Focus of that review is the incorporation of uncertainties into fatigue crack growth models and structural reliability assessment with first-order reliability methods, exemplified on a jacket structure. Interesting for circumferential welds in OWT towers and monopiles is the contribution by Li et al. [11] who evaluated fatigue reliability of berthing monopiles based on a fracture mechanics approach and developed stress intensity and concentration factors for circumferential butt welds.

The major difference between jacket-supported oil & gas platforms and OWTs is the dynamic response which plays a significantly larger role for OWTs due to wind excitation [12]. Dong et al. [12] emphasize that larger uncertainties are present in the hot spot stress for tubular joints for OWTs compared to oil & gas platform jackets. So far, only a few publications are available that applied a linear-elastic fracture mechanics model on OWT support structures. Dong et al. [13] base fatigue reliability analysis of jacket supported OWTs on a fracture mechanics model which also accounts for corrosion by fitting 2-parameter Weibull and Gamma functions to obtain a long-term distribution of hot spot stress ranges. In [14–16] a fracture mechanics approach is used for risk-based planning of operation and maintenance of OWTs. These authors compare calculated reliability values with inspection outcomes during operation, taking into account the probability of crack detection. All authors calibrate the parameters of their fracture mechanics models (e.g. material parameters C and m, initial crack size a_0) so that it yields an identical reliability level over time as calculated in the SN-curve analysis. Yeter et al. [17] consider initial crack size and selected material characteristics as random variables and apply a fracture mechanics model to update structural reliability based on inspections and repair. Finally, Márquez-Domínguez & Sørensen [18] calibrate fatigue design factors of support structures with a fracture mechanics model.

To the knowledge of the authors, there is no published work that addresses the effect of the sequence of loading and weather seasonality on fatigue crack growth for offshore wind jackets, although studies on other applications have shown that subsequent load peaks might cause acceleration and retardation of crack growth [19–22]. Additionally, there is a need to critically assess the difficulties of a fracture mechanics model for OWT jackets concerning lifetime prediction: what are suitable parameterization approaches, and how sensitive are crack growth results to changes in the model parameters?

2. FATIGUE DESIGN METHODS

The fatigue life of a component can be categorized into three phases: (1) microstructural processes leading to *crack initiation*, (2) continuous *crack propagation* and (3) accelerated crack growth ending in *brittle failure* [23]. A fatigue crack initiates at the hot spot point of the structure, typically due to small welding defects in combination with stress concentration and weld geometry [7]. Hot spots are structural locations with the highest expected cumulative damage over the lifetime.

Fatigue analysis can be based on either SN-curves (cf. Section 2.1) or fracture mechanics (cf. Section 2.2). Industry practice for fatigue design of OWT support structures is the use of SN-curves, which is also recommended in standards applicable to OWT support structure design [7,24]. SN-curves quantify material resistances to fatigue loading in terms of number of constant amplitude stress cycles until failure. Failure is defined as through-thickness crack [7]. Therefore, all three fatigue phases from crack initiation until fracture are only represented with a single curve in the SN-approach. However, to include information from inspection and monitoring, a model that describes fatigue crack growth in terms of measurable damage is needed.

Fracture mechanic models provide solutions as they describe crack growth as function of stress cycles, structural and crack geometry, and material parameters. These models typically depict the second fatigue phase only (crack propagation), assuming that an initial crack is already existing in the structure. Fracture mechanic approaches are recommended as a supplement to SN-curves in industry guidelines [7,24]. Both guidelines refer to [25] for detailed guidance on fatigue assessment with fracture mechanics.

2.1 SN-curve design

SN-curves are generated from fatigue testing of small material specimen. SN-curves are specified as piecewise-linear curves with one or two segments. Parameterization of the applicable SN-curve depends on the type of weld connection and environment, e.g. air, seawater with cathodic protection, or seawater with free corrosion. Recommendations for design SN-curves are given in industrial guidelines such as [7,24,26]. Design SN-curves typically refer to mean-minus-two-standard-deviation curves from experimental data corresponding to a 97.7% probability of survival [7]. Circumferential butt welds (also called girth welds) connecting the tower sections of OWTs must be welded from both sides according to DNV [24]. The most frequently used SN-curve for this welding connection is "detail category D" specified in [7]. Tubular joints, such as the connection of jacket brace to leg, are assessed with the SN-curve "T" [7].

Fatigue damage is commonly calculated with the Palmgren-Miner hypothesis of linear damage accumulation. This rule specifies fatigue damage D as the ratio of occurred stress cycles n_i (given by load history) to number of stress cycles until failure N_i (given by SN-curve), summed up over all occurring stress ranges $i=1,2,\ldots$ as shown in Eq. 1 [27]. The structure is designed to withstand fatigue loading if D<1 over the lifetime.

$$D = \sum_i \frac{n_i}{N_i} \tag{1}$$

Recently, Brennan & Tavares [28] criticized that databases for SN-curves are out of date and do not represent current knowledge in several areas, such as regarding corrosion, but also advanced fabrication, quality control, and inspection techniques. Additionally, studies have shown that the sequence, in which loading occurs, influences fatigue crack growth, which is neglected in the linear damage accumulation hypothesis [19–21].

2.2 Fracture mechanics

Crack propagation relationships are derived from experimental test results of crack growth in material specimen exposed to (constant amplitude) loading. Several models exist, of which the most frequently applied model is Paris' law presented in Eq. 2 and 3 [29]. According to Paris' law, the crack growth increment da per load cycle dN follows an exponential function with stress intensity factor ΔK_I and the material constants C and m. The material constants are determined empirically. Several standards and practices give guidance on parameter selection [7,24,25].

$$\frac{da}{dN} = C(\Delta K_I)^m \tag{2}$$

Numerical solutions based on finite element modelling for the stress intensity factor ΔK_I are most accurate but involved and computationally demanding. Therefore, analytical solutions are provided by standards which are deduced from semi-elliptical cracks in plates [25].

The stress intensity factor ΔK_I can be calculated as a function of the stress ranges ΔS and a geometry factor Y (cf. Eq. 3), which depends on crack and structural geometry as well as loading type [30].

$$\Delta K_I = \Delta S \cdot Y \cdot \sqrt{\pi \cdot a} \tag{3}$$

Typically, there is a minimum threshold stress intensity factor ΔK_{th}, below which the stress cycles are assumed to not contribute to crack propagation. Alternatively to Eq. 2, the offshore standard DNV-OS-J101 [24] recommends the crack growth relationship in Eq. 4, which leads to less conservative results for identical material parameters. The recommended threshold value is $\Delta K_{th} = 79.1\ MPa\sqrt{mm}$ [24].

$$\frac{da}{dN} = C(\Delta K_I{}^m - \Delta K_{th}{}^m) \tag{4}$$

Equation 4 leads to smaller crack growth rates, especially if there are a large number of stress intensity factors near the threshold value, which is the case for OWTs where the high-cycle fatigue region is dominant. Equation 4, however, deviates from BS 7910 [25] which recommends Eq. 5 as less conservative version of Eq. 2, where R is the stress ratio for welded joints. R is defined as ratio of minimum to maximum absolute stress level [25].

$$\frac{da}{dN} = C\left(\frac{\Delta K_I - \Delta K_{th}}{1-R}\right)^m \tag{5}$$

According to DNV GL [7], the fatigue life calculated with fracture mechanics shall be shorter than the one derived with SN-curves since the time for crack initiation is included in SN-curves but assumed to already have happened in fracture mechanics modelling. Fatigue failure in fracture mechanics models is expressed according to a critical crack depth a_c. Criteria for a_c used in previous studies are wall thickness t, $t/2$, or a function of fracture toughness, geometry function and average stress range as specified by Li et al. [11].Fracture mechanics models are applied at structural hot spots, where cracks are assumed to happen first. The stress ranges ΔS required for fatigue crack assessment with Eq. 2 are hot spot stresses which are specific for the considered crack opening mode. Hot spot stresses are derived through superposition of nominal stresses from axial loading, in-plane and out-of-plane bending, which are weighted with a stress concentration factor. Hot spot stresses are typically evaluated at eight locations from crown toe to saddle to crown heel of welded joints, with linear interpolation, as shown in Fig. 1 for a Y-joint connection between jacket leg and brace. In this study, the formulas given in [7] for tubular joints are applied.

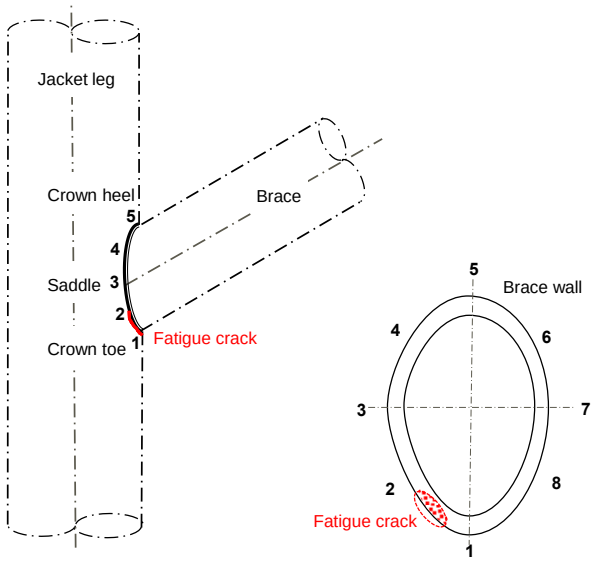

FIGURE 1. Y-joint between jacket leg and brace with eight hot spot locations and fatigue crack with semi-elliptical shape.

OWTs are subjected to variable-amplitude loading, which follows an annual trend, since wind and wave characteristics are influenced by weather seasonality. There are two impacts of loading sequence on fatigue crack growth: (1) a mathematical effect based on the non-linearity of Eq. 2 and 3, and (2) a physical effect, as over-load causes crack growth retardation.

The mathematical effect is due to the Eq. 2: the crack growth per load cycle for the time step *i* depends on the crack depth in the previous time *i-1*. Consequently, the sequence, in which stress ranges occur, has the following effect in a given time series: The overall crack growth is larger if high stress ranges occur early and lower stress ranges later in time than vice versa.

The physical effect that crack growth retards after application of high tensile load cycles has been observed in experiments with variable-amplitude loading and is explained with either a crack-closure theory or crack-tip plasticity approach [31]. This paper studies the mathematical effect, especially regarding weather seasonality, but excludes physical growth retardation theories since these depend on crack geometry and plastic zone characteristics that are affected by large uncertainties.

2.3 Calibration of fracture mechanic models

As an alternative to the empirical determination of material constants by accelerated fatigue testing, these parameters can be calibrated using results of SN-curve analysis. This calibration is beneficial if the structure is initially designed using the SN-approach, however a detailed lifetime reassessment is required after some years in operation, e.g. due to additional available information from on-site inspections or monitoring of loads and/or environmental factors. Calibration can be stochastic or semi-empirical. Stochastic calibration accounts for the uncertainty in fatigue crack growth by randomizing parameters such as initial crack size and geometry function [9,34]. The material parameter *m* is often taken with a fixed value, while *C*

TABLE 1. Typical parameters used in fracture mechanics models with Paris' law for tubular joints on OWT jackets and other structures. Studies referring to OWT jackets are marked with the superscript OWT. The mean value μ and standard distribution σ are given for a normal distribution of the parameter ln(C) (natural logarithm of C).

m [-]	$\mu_{\ln(C)}$ $\left[\frac{mm}{(MPa\sqrt{mm})^m}\right]$	$\sigma_{\ln(C)}$ $\left[\frac{mm}{(MPa\sqrt{mm})^m}\right]$	**Dist**	K_{th} $MPa\sqrt{mm}$	**Source**
3.1	-29.84	0.55	-	79.1	[24]OWT
3.42	-30.56	0.58	-	63	[25][1]
1.11	-14.38	0.14	-	63	[25][2]
refers to [25]					[7]
3.1	-29.84	0.55	N	-	[13] OWT
2.88	-28.16	0.66	N	-	[17] OWT
3	-29.75	0.5	N	190-144R	[9]
3	-26.13	0.119	N	-	[32][3]
3	-29.24	0.55	N	100	[33][3]
2.55	-27.77	0.003	N	-	[14] (OWT)4

Abbreviations and variables used in the table: Dist: distribution type, N: normal distribution, μ: mean value, σ: standard deviation. The parameters given are for tubular joints in seawater with corrosion protection, if not specified otherwise. [1,2] [25] specifies a two-slope relationship with two parameter sets (valid for R≥0.5 and cathodic protection at -850 mV). [3]Authors do not specify if corrosion protection is applied. [4]Parameters m and ln(C) are fitted to SN-curve reliability for a gearbox example.

is assumed as a lognormal or normal distributed variable. Characteristic values of *m* and *C* from literature are presented in Tab. 1. The majority of sources apply a one-slope relationship between stress intensity factor ΔK_I and crack growth *da/dN* apart from the standard BS 7910 [25]. The material parameters are mostly in the same order of magnitude, while there is no consent about implementation of threshold values for stress intensity factors ΔK_{th}. According to DNV [24], *C* should be applied in crack growth models as mean plus two standard deviations from test results.

Semi-empirical calibration uses results from SN-curve analysis, such as the reliability level over time to fit unknown constants, typically *C* and *m*, in the fracture mechanic models [13–16]. This changes the meaning of *C* and *m* from originally material constants to model effective parameters. In this paper, *C* was calibrated to yield an identical fatigue life as the SN-curve analysis. The 20-year damage value *D* obtained with the Palmgren-Miner rule of linear damage accumulation was extrapolated until the failure condition *D=1*. The corresponding lifetime until failure $T_{failure}$ is input for the fracture mechanics calibration, where *C* is adjusted until the crack depth at $T_{failure}$ equals the critical crack depth a_c. In this study, a_c is chosen as through-thickness crack of the brace wall thickness ($a_c=t_{brace}$) as this corresponds to the failure criteria of the SN-curve (*D=1*) [7].

2.4 Wind turbine model and load simulation

The OWT assembly studied in this paper (cf. Fig. 2) consists of the NREL 5 MW reference turbine [35] supported by the UpWind jacket structure which was used in the OC4 project [36]. The OC4 jacket structure was implemented as a finite-element model in the flexible multibody solver FEDEM Windpower (Version 7.1; Fedem Technology AS, Trondheim) using Euler-Bernoulli beam theory. Structural properties of jacket legs, braces and joints were kept identical to OC4 specifications. A summary of the jacket and tower dimensions is given in Tab. 2. For detailed information on the jacket structure reference is made to Vorpahl et al. [37]. The original jacket model was extended to include a distributed spring model for soil-pile interaction in accordance with API [26]. The jacket is located on a typical site in the North Sea with 50m water depth.

OWTs are highly dynamic systems making the support structure prone to fatigue failure. Due to its modal properties the jacket support structure is especially sensitive to excitation from the wind turbine rotor. Therefore, loading is analyzed in this study for the fatigue relevant load cases of power production and parked (idling) condition according to IEC [38]. In total 15 load cases were defined with wind speeds from 2 m/s until 30 m/s in steps of 2 m/s. The load cases 4 m/s until 24 m/s represent operational conditions, while the remaining ones are idling. The lumped sea states given in the UpWind Design Basis [39] are allocated to each wind speed. Wind and waves were unidirectional during the simulations. Current and yaw-misalignment was neglected. The occurrence of each load case is linked to the wind speed distribution. Long-term wind conditions (mean wind speed) were simulated with a Markov weather model which was calibrated with historical data as explained in the following section. Short-term variations of wind speed (turbulences) are modeled with the stochastic inflow turbulence tool TurbSim (Version 1.06.00, NREL, Colorado) by applying the Kaimal turbulence spectrum according to specifications in the OC4 project.

Aerodynamic and hydrodynamic loads on the OWT from each load case were simulated decoupled from each other in order to speed up the analysis. Aerodynamic loads (forces and moments at tower top) were simulated with a flexible rotor model (according to the NREL 5MW turbine) on a rigid support structure. Hydrodynamic loads were calculated as integrated load time series at mean sea level that yield an equivalent bending moment at mudline. To account for dynamic interaction between rotor and support structure, aerodynamic damping was added in the hydrodynamic load simulation. Aerodynamic damping was modeled with a viscous damper at tower top with a constant damping ratio as 4 % of the critical damping of the first mode [40].

The structural response to environmental loading was calculated with impulse based substructuring. This technique uses the principle of superposition of impulse responses for a linear system [41] and was further developed in [42] for application to OWTs. A brief summary of the applied method is given in the following. For details and proof of accuracy reference is made to Schafhirt et al. [43].

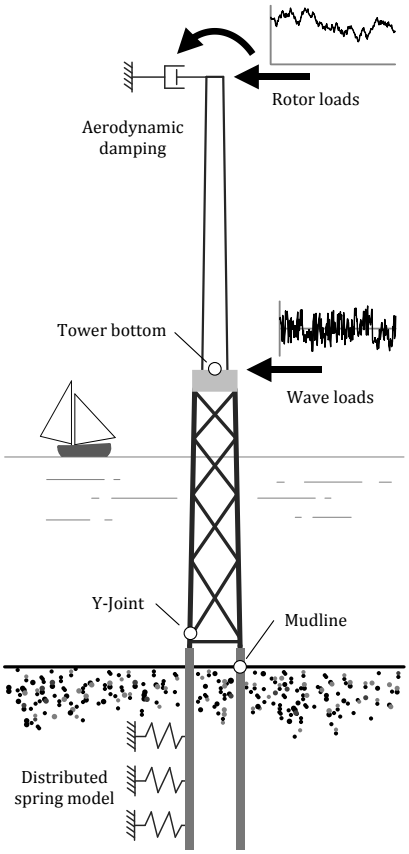

FIGURE 2. Model of jacket support structure used in this study.

TABLE 2. Summary of support structure dimensions: diameter D_S and wall thickness t of tower and jacket.

	Tower top	Tower bottom	Jacket leg top/ mid-braces	Jacket leg bottom	Jacket brace	Jacket pile
D_S [m]	4	5.6	1.2	1.2	0.8	2.082
t [mm]	30	32	40/ 35	50	20	60

In this study, small impulse loads were applied to the tower top (wind loads, six degrees of freedom) and mean sea level (wave loads, one degree of freedom) to obtain impulse response functions [43]. Computational effort is linearly increasing with the number of input degrees of freedom. Wave loads were applied in one degree of freedom only (fore-aft) to increase computational efficiency since their effect towards the other coordinates is assumed to be minor. The dynamic response of the jacket structure is dominated by wind-induced loads; hence these were represented in the complete coordinate set. FEDEM Windpower was used to pre-compute hydrodynamic and aerodynamic loads and to simulate the impulse response functions in the time-domain.

Structural response at specified output locations (tower bottom, mudline, Y-joint) was then determined by convoluting the

impulse response functions with environmental load time series. For each load case, a 1h time series of structural response was simulated. This is equivalent to six 10-minute simulations with different random realizations in order to account for statistical uncertainty.

2.5 Markov weather model

Wind speeds occurring during the lifetime of the support structure are simulated with a Markov weather model [44]. This model enables the simulation of realistic time-dependent wind speed sequences where also annual weather seasonality is represented adequately. The weather model generates a persistent wind speed time series with the assumption of finite memory (Markovian property): current wind speeds during a time step depend only on wind speeds during the previous time step.

The transition probabilities from one state (here: wind speed) to the subsequent one are collected in a Markov matrix which was set up from historical data [45]. States were chosen according to the load case definitions (2 m/s until 30 m/s in steps of 2 m/s).

Historical wind data in 6 h resolution over 22 years from the European Centre for Medium-Range Weather Forecasts was used as it is conveniently accessible for various locations [46]. Figure 3 presents the yearly wind speed distribution of the historical data for a location in the North Sea near the UK coast. Transition matrices were calculated for each month in order to capture the weather seasonality that is present in the data. The monthly mean wind speeds averaged from 22 years of data are presented in Fig. 4. The maximum difference in monthly mean wind speed is over 3m/s during a year.

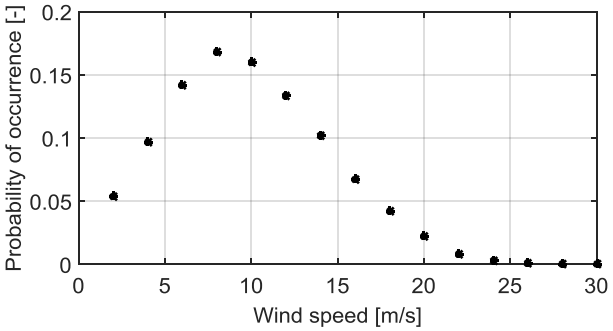

FIGURE 3. Yearly wind speed distribution from historical data.

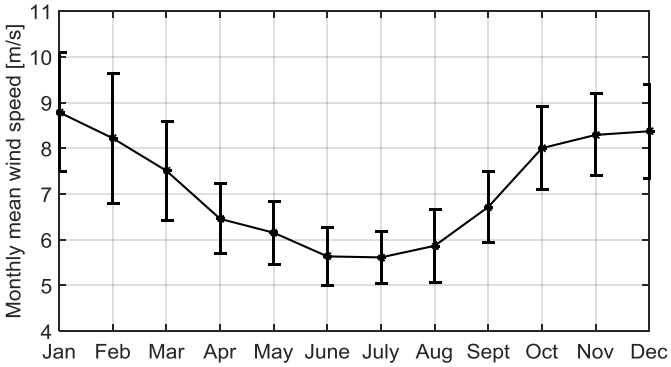

FIGURE 4. Monthly mean wind speeds averaged from 22 years of historical data. Monthly standard deviations are given with error bars.

TABLE 3. Applied data for SN-curve and fracture mechanics model for fatigue design of OWT jacket.

Parameter	Unit	Value	Source
SN-curve for Y-joint	-	"T" seawater corrosion protection	[7]
m_1	-	3.0	[7]
m_2	-	5.0	[7]
$\log a_1$	-	12.164	[7]
$\log a_2$	-	15.606	[7]
SCF	-	cf. [7] Annex B	[7]
FM model for Y-joint			
a_0	*mm*	0.1	[24]
a_c	*mm*	20 (=t_{brace})	[11,13]
m	-	3.1	[24]
ln(C)	$\frac{mm}{(MPa\sqrt{mm})^m}$	-29.33	calibrated
Y	-	1	[9]
K_{th}	$MPa\sqrt{mm}$	0	[13,16,17]

2.6 Damage and crack analysis

Rainflow-counting was performed on the structural response time series to obtain the stress ranges ΔS_i and number of cycles n_i. Hot spot stresses were calculated at eight locations of the Y-joint and serve as input in the SN-curve analysis and fracture mechanics model. The hot spot stresses were additionally multiplied with a geometry function for calculation of the stress intensity factor used in the fracture mechanics model.

In the SN-curve analysis, the number of hot spot stress cycles for each load case was scaled with the occurrence probability of this load case during the lifetime, based on the wind distribution (cf. Fig. 2). Damage was then calculated with Eq. 1.

A wind time series with lifetime duration and 6h resolution was simulated for the fracture mechanics analysis. A stress range sequence for the full lifetime was then set up by using in succession the n_i-ΔS_i pairs from the load case corresponding to the wind time series. Crack growth was then calculated with Eq. 2 and 3.

The parameters used in the damage and crack analysis are presented in Tab. 3. No threshold value for the stress intensity factor K_{th} was implemented, leading to conservative results.

3. RESULTS

3.1 SN-curve results

Results of the SN-curve analysis for the fatigue critical hot spot in the Y-joint are presented in Fig. 5. This hot spot is located at the intermediate point between saddle and crown toe of the welded joint. The hot spot stress ranges for 20 years of load

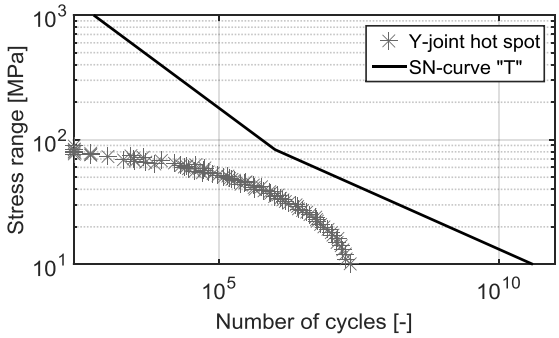

FIGURE 5. Hot spot stress at Y-joint occurring during 20 year lifetime of the jacket and the design SN-curve "T".

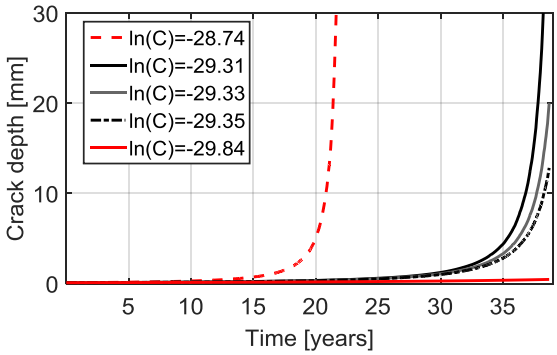

FIGURE 6. Crack growth under various *C* parameters with random weather occurrence.

simulation are lumped into bins with a distance of 1 MPa. It can be seen that most of the damage is caused by high-cylce fatigue ($N>10^5$). The damage-value for a lifetime of 20 years is *D=0.516*. Consequently, the extrapolated lifetime until failure (*D=1*) is 38.79 years for this hot spot (linear extrapolation).

3.2 Fracture mechanics calibration

The same hot spot of the Y-Joint was then analysed with the fracture mechanics model. Figure 6 shows the crack growth over the total lifetime until failure (38.79 years) for various values of the *C* parameter. The wind time series was generated by random sampling from the wind distribution, therefore the loading sequence is random in time. This wind distribution and all other parameters apart from *C* are kept identical for the different crack simulations. A value of *ln(C)=-29.33* leads to the correct critical crack size a_c after 38.79 years. This value is in between the results with using the material value from DNV [24] (here marked in red), where the more conservative line (dashed) corresponds to the mean plus two standard deviations, while the other one is based on the mean value only (cf. Tab. 1). The figure shows that small variations in the *C* parameter lead to strong deviations in the fatigue crack growth rate closer to the end of the lifetime, while less deviation can be seen up to a crack depth of 3mm.

The crack growth results also depend strongly on the initial crack size a_0 (not shown here). An increase of initial crack size causes a shift of the crack depth curve in time.

3.3 Sequence of loading

The calibrated fracture mechanics model was then used to study the effect of weather seasonality on fatigue crack growth. Figure 7 presents fatigue crack growth for a persistent wind time series in comparison with a time series with random weather occurrence. The persistent wind time series was generated with the Markov weather model (cf. Section 2.5). In the random time series, the occurrence of the wind speed states is kept identical to the persistence wind time series, however their order is randomized. This randomization deletes weather persistence and seasonality in the time series.

The final crack depth at the end of the lifetime is identical for both weather simulations. However, a zoom in to the marked area (cf. Fig. 8) shows clearly the effect of seasonal weather trends: fatigue crack growth accelerates during the winter period, while it decelerates during the other half of the year.

500 Monte Carlo simulations of fatigue crack growth with lifetime duration were run to analyse the statistical properties of the crack size distributions at the end of lifetime for the Y-joint. Results were compared for weather simulation with (I) the Markov weather model and (II) a random weather model. The random weather model samples wind state occurrences randomly from the historical long-term wind speed distribution (cf. Fig. 3). Consequently, the wind state in time step *i* is independent of the previous time step *i-1* (no persistence, no seasonality). 500 Monte Carlo simulations lead approximately

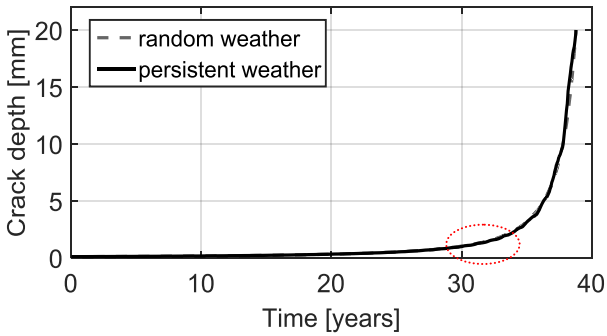

FIGURE 7. Crack growth under random weather occurrence and persistent weather simulation with annual seasonality. A zoom into the area marked red is presented in Fig. 8.

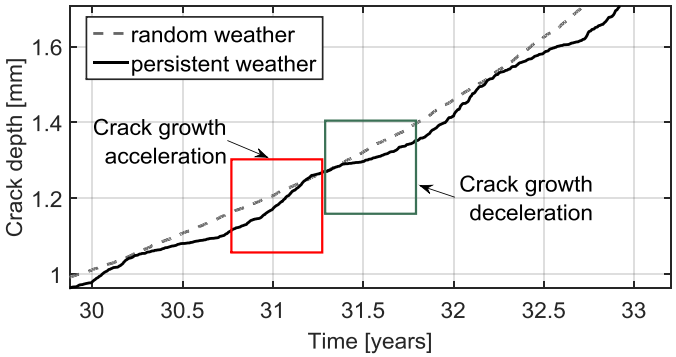

FIGURE 8. Zoom into Fig. 7 for visualization of the seasonality effect on fatigue crack growth.

to an accuracy of +/ 0.46 mm of the estimate of mean crack depth calculated with persistent wind.
Results are presented in Fig. 9 and Tab. 4. The Markov weather model leads to a larger standard deviation of the final crack depth and the distribution is skewed to higher crack depth compared to the random weather simulation.

4. DISCUSSION

The results presented in Chapter 3 have shown that the fracture mechanics model enables a more detailed analysis of material deterioration, such as accounting for weather seasonality, compared to the SN-curve approach. Nevertheless, modelling of crack growth is highly involved and results are much dependent on assumptions regarding parameterization and initial crack size. The validity of these assumptions has therefore a large influence on the accuracy of the lifetime prediction.
Semi-empirical calibration of fracture mechanic parameters is possible in order to match the model with the SN-curve lifetime prediction. This calibration is only valid for the chosen set of parameters.

4.1 Opportunities

Fatigue cracks are an observable phenomenon on the support structure which can be measured in contrast to the damage result of the SN-curve approach, which is a percentage value not related to an explicit physical state (apart from *D=1* stating failure). This enables to update lifetime predictions and reliability through results from on-site inspections like several authors have shown [12,14–16,32].
Prediction updates are valuable for optimization of inspection rhythms, since close visual underwater inspections are very expensive and involve high risk with diving operations [47]. An identical safety level can be achieved with either larger design safety factors or more frequent inspections. DNV [24] links periodic inspections intervals to the magnitude of design and material safety factor applied in the design. This leads to a pareto-optimal solution between minimization of design conservatism and number of inspections.
The exponential crack growth relationship makes inspections more relevant at the end of the service life, since deviations of crack growth due to parameter uncertainty of *C* are only visible from 15 years on (cf. Fig. 6). In addition, an early inspection might be needed to confirm that there were no undetected material defects from fabrication leading to initial crack sizes that exceed design assumptions.
For a detected crack, the remaining lifetime until fracture can be calculated for decisions about needed repair or allowed operational loads to prevent or delay failure.

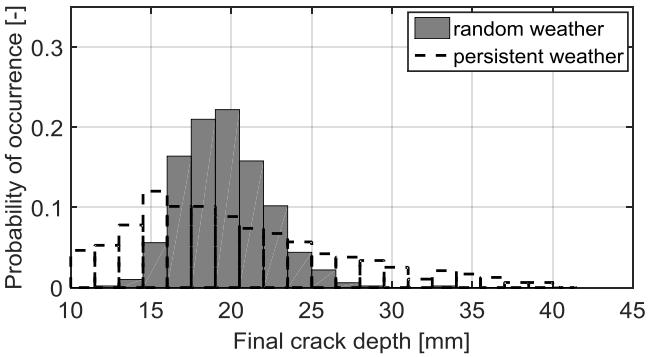

FIGURE 9. Distribution of final crack depth after 38.79 years calculated with random and persistent wind occurrence.

TABLE 4. Statistical properties of distribution of final crack depth $a_{lifetime}$ calculated with random wind and persistent wind occurrence.

Property	$a_{lifetime}$ [mm] of random wind	$a_{lifetime}$ [mm] of persistent wind
Mean	19.57	21.66
Standard deviation	2.68	10.36
Skewness	0.62	3.62

4.2 Challenges

The main challenge is the accurate prediction of fatigue crack growth, which is a stochastic phenomenon. Diverging recommendations of material parameters and initial crack sizes show that there is no agreement about fracture mechanics model implementation. The inherent randomness of material fatigue requires probabilistic analysis; however quantification of uncertainties is a challenge where long-term operational experiences in the offshore wind industry are missing.
Further development is needed to properly include corrosion into crack growth analysis since typical approaches are based on engineering assumptions instead of empirical tests [28]. Lifetime prediction needs to not only account for deterioration but also for maintenance processes like repair of corrosion protection or fatigue cracks where practices on how to model that are needed.
Kirkemo [9] hypothesises that 90 % of structural failures occur due to gross error in design. The fracture mechanics approach is more complex than SN-curve design which increases the risk of gross errors.
The probability of detection of a fatigue crack is low for small crack sizes. Additionally, for larger and therefore better detectable fatigue cracks, the crack growth rate accelerates rapidly. Consequently, there is only a small time window for detection and repair of cracks before failure. This makes it difficult to update lifetime estimates based on inspection results during most of the fatigue lifetime; however makes fracture mechanics an attractive approach for decision about lifetime extension of OWTs.

5. CONCLUSION AND OUTLOOK

Opportunities and challenges of crack growth modelling have been discussed in this paper based on a simplistic fracture mechanics model. The examples of parameter calibration and

weather seasonality indicate that detailed modelling of crack growth plays an important role once OWTs approach the end of their design lifetime. Crack growth was predicted conservatively by neglecting the threshold value for the stress intensity factor. The crack growth prediction can be made more realistic by advanced modelling of the stress intensity factor and by including a threshold value.

This paper is restricted to analyse crack growth due to selected load cases of power production and idling only. In industry application, lifetime prediction needs to account for all relevant load cases and other deterioration processes (such as fatigue during installation and from vessel impact). In addition, the relevance of crack growth retardation due to overload should be studied for OWTs.

The semi-empirical calibration of fracture mechanic parameters can be improved through implementation of a probabilistic analysis in order to account for the random nature of fatigue. Additionally, a two-parameter calibration of *C* and *m* should be considered.

Future work is required to refine the suggested approach for more accurate crack growth predictions. In addition, further research on the effect of corrosion and the validation of crack growth models based on operational data of OWTs is needed.

ACKNOWLEDGMENTS

This project has received funding from the European Union's Horizon 2020 research and innovation programme under the Marie Sklodowska-Curie grant agreement No 642108. It is acknowledged that the OC4 load simulations were provided by Sebastian Schafhirt, Norwegian University of Science and Technology, Trondheim.

REFERENCES

[1] European Wind Energy Association, 2013,"Deep water – the next step for offshore wind energy," Brussels.

[2] Corbetta G., Pineda I., Moccia J., and Guillet J., 2014,"The European offshore wind industry - key trends and statistics 2013," European Wind Energy Association, Brussels.

[3] IEA Wind, 2015,"2014 Annual report," International Energy Agency, Paris.

[4] Offshorewind,"Samsø Turbine Broke Off Due to Welding Crack," http://www.offshorewind.biz/2015/12/15/samso-turbine-broke-off-due-to-welding-crack/. Accessed on 27.12.2015.

[5] Vorpahl F., Schwarze H., Fischer T., Seidel M., and Jonkman J., 2013,"Offshore wind turbine environment, loads, simulation, and design," WENE, **2**(5), pp. 548–570.

[6] Ziegler L., Voormeeren S., Schafhirt S., and Muskulus M., 2015,"Sensitivity of Wave Fatigue Loads on Offshore Wind Turbines under Varying Site Conditions," Energy Procedia, **80**, pp. 193–200.

[7] DNV GL, 2014,"Fatigue design of offshore steel structures," Recommended practice RP-C203.

[8] Qian X., 2016, Fracture representation and assessment for tubular offshore structures, *Handbook of Materials Failure Analysis with Case Studies from the Oil and Gas Industry*, Elsevier, pp. 371–392.

[9] Kirkemo F., 1988,"Applications of Probabilistic Fracture Mechanics to Offshore Structures," Appl. Mech. Rev., **41**(2), p. 61.

[10] Shetty N. K., and Baker M., 1990,"Fatigue reliability of tubular joints in offshore structures: Crack propagation model," *Proceedings of Int. Offshore Mechanics and Arctic Eng. Symposium*, pp. 223–230.

[11] Li Y., Lence B. J., Shi-Liang Z., and Wu Q., 2011,"Stochastic Fatigue Assessment for Berthing Monopiles in Inland Waterways," J. Waterway, Port, Coastal, Ocean Eng., **137**(2), pp. 43–53.

[12] Dong W., Moan T., and Gao Z., 2011,"Statistical Uncertainty Analysis in the Long-Term Distribution of Wind- and Wave-Induced Hot-Spot Stress for Fatigue Design of Jacket Wind Turbine Based on Time Domain Simulations," *ASME 2011 30th International Conference on Ocean, Offshore and Arctic Engineering*, pp. 407–417.

[13] Dong W., Moan T., and Gao Z., 2012,"Fatigue reliability analysis of the jacket support structure for offshore wind turbine considering the effect of corrosion and inspection," Reliability Engineering & System Safety, **106**, pp. 11–27.

[14] Sørensen J. D., 2009,"Framework for risk-based planning of operation and maintenance for offshore wind turbines," Wind Energ., **12**(5), pp. 493–506.

[15] Rangel-Ramírez J. G., 2010,"Reliability Assessment and Reliability-Based Inspection and Maintenance of Offshore Wind Turbines," Aalborg University, Aalborg, Denmark.

[16] Nielsen J. S., 2013,"Risk-based operation and maintenance of offshore wind turbines," PhD thesis, Aalborg University, Aalborg, Denmark.

[17] Yeter B., Garbatov Y., and Guedes Soares C., 2015,"Fatigue reliability of an offshore wind turbine supporting structure counting for inspection and repair," *Proceedings of the 5th International Conference on Marine Structures*, CRC Press/Balkema.

[18] Márquez-Domínguez S., and Sørensen J. D., 2012,"Fatigue Reliability and Calibration of Fatigue Design Factors for Offshore Wind Turbines," Energies, **5**(12), pp. 1816–1834.

[19] Wheeler O. E., 1972,"Spectrum Loading and Crack Growth," J. Basic Engineering, **94**(1), p. 181.

[20] Verma B. B., and Pandey R. K., 1999,"The effects of loading variables on overload induced fatigue crack growth retardation parameters," Journal of Materials Science, **34**(19), pp. 4867–4871.

[21] Mohanty J. R., Verma B. B., and Ray P. K., 2008,"Evaluation of overload-induced fatigue crack growth retardation parameters using an exponential model," Engineering Fracture Mechanics, **75**(13), pp. 3941–3951.

[22] Maljaars J., Pijpers R., and Slot H., 2015,"Load sequence effects in fatigue crack growth of thick-walled welded C–

Mn steel members," International Journal of Fatigue, **79**, pp. 10–24.
[23]Stephens R. I., and Fuchs H. O., 2000. *Metal fatigue in engineering*, 2nd ed., J. Wiley, New York.
[24]Det Norske Veritas, 2014,"Design of offshore wind turbine structures.," Offshore standard DNV-OS-J101.
[25]British Standard Institution, 2005,"Guide on methods for assessing the acceptability of flaws in fusion welded structures," BS 7910.
[26]American Petroleum Institute, 2000,"Recommended practice for planning, designing and constructing fixed offshore platforms—working stress design," Recommended practice RP 2A-WSD.
[27]Petersen C., 2013. *Stahlbau*, Springer Fachmedien Wiesbaden, Wiesbaden.
[28]Brennan F., and Tavares I., 2014,"Fatigue design of offshore steel mono-pile wind substructures," Proceedings of the ICE - Energy, **167**(4), pp. 196–202.
[29]Paris P., and Erdogan F., 1963,"A Critical Analysis of Crack Propagation Laws," J. Basic Engineering, **85**(4), p. 528.
[30]Raju I. S., and Newman J. C., 1979,"Stress-intensity factors for a wide range of semi-elliptical surface cracks in finite-thickness plates," Engineering Fracture Mechanics, **11**(4), pp. 817–829.
[31]Lee S. Y., Sun Y., An K., Choo H., Hubbard C. R., and Liaw P. K., 2010,"Evolution of residual-strain distribution through an overload-induced retardation period during fatigue-crack growth," J. Appl. Phys., **107**(2).
[32]Aghakouchak A. A., and Stiemer S. F., 2001,"Fatigue reliability assessment of tubular joints of existing offshore structures," Can. J. Civ. Eng., **28**(4), pp. 691–698.
[33]Walbridge S., and Nussbaumer A., 2007,"A probabilistic model for determining the effect of post-weld treatment on the fatigue performance of tubular bridge joints," International Journal of Fatigue, **29**(3), pp. 516–532.
[34]Byers W. G., Marley M. J., Mohammadi J., Nielsen R. J., and Sarkani S., 1997,"Fatigue Reliability Reassessment Applications: State-of-the-Art Paper," Journal of Structural Engineering, **123**(3), pp. 277–285.
[35]Jonkman J., Butterfield S., Musial W., and Scott G., 2009,"Definition of a 5-MW reference wind turbine for offshore system development," National Renewable Energy Laboratory, Goldon, CO.
[36]Popko W., et al. 2012,"Offshore Code Comparison Collaboration Continuation (OC4), Phase 1 - Results of Coupled Simulations of an Offshore Wind Turbine With Jacket Support Structure," *Proceedings of The Twenty-second International Offshore and Polar Engineering Conference*.
[37]Vorpahl F., Popko W., and Kaufer D., 2011,"Description of a basic model of the "UpWind reference jacket" for code comparison in the OC4 project under IEA Wind Annex 30," Fraunhofer Institute for Wind Energy and Energy System Technology, Germany.
[38]International Electrotechnical Commission, 2009,"Wind turbines – part 3: Design requirements for offshore wind turbines," International standard IEC 61400-3.
[39]Fischer T., De Vries W. E., and Schmidt B., 2010,"UpWind design basis," WP4: Offshore foundations and support structures, UpWind.
[40]Salzmann D. J. C., and Van der Tempel J., 2005,"Aerodynamic damping in the design of offshore support structures for offshore wind turbines," *Proceedings of the European Offshore Wind Conference*, Brussels.
[41]Clough R. W., and Penzien J., 1975. *Dynamics of structures*, McGraw-Hill, New York.
[42]van der Valk P., and Rixen D., 2012,"Impulse Based Substructuring for Coupling Offshore Structures and Wind Turbines in Aero-Elastic Simulations," *53rd AIAA/ASME/ASCE/AHS/ASC Structures*, pp. 1–14.
[43]Schafhirt S., Verkaik N., Salman Y., and Muskulus M., 2015,"Ultra-fast analysis of offshore wind turbine support structures using impulse based substructuring and massively parallel processors," *Proceedings of The Twenty-fifth International Offshore and Polar Engineering Conference*.
[44]Scheu M. N., Matha D., and Muskulus M., 2012,"Validation of a Markov-based Weather Model For Simulation of O&M For Offshore Wind Farms," *Proceedings of The Twenty-second International Offshore and Polar Engineering Conference*.
[45]Anastasiou K., and Tsekos C., 1996,"Persistence statistics of marine environmental parameters from Markov theory, Part 1: Analysis in discrete time," Applied Ocean Research, **18**(4), pp. 187–199.
[46]European Centre for Medium-Range Weather Forecasts, http://www.ecmwf.int/.
[47]Moan T., Vardal O. T., and Johannesen J. M., 1999, Probabilistic inspection planning of fixed offshore structures, *ICASP 8, Applications of Statistics and Probability*, Rotterdam, Netherlands, pp. 91–200.